TECHNISCHE MECHANIK, Band 28, Heft 3-4, (2008), 237 – 258
Manuskripteingang: 24. Oktober 2007

Dynamic Response of Prestressed Timoshenko Beams Resting on Two-Parameter Foundation to Moving Harmonic Load

Nguyen Dinh Kien

The dynamic response of prestressed Timoshenko beams fully and partially resting on a two-parameter elastic foundation to a moving harmonic load is investigated by the finite element method. A beam element with shear deformation taking the effect of prestress and foundation support for the dynamic analysis is formulated in the context of the field consistent approach. Using the formulated element, the dynamic response of the beams having different boundary conditions is computed by using the direct integration Newmark method. The effects of prestress, foundation support, moving velocity and excitation frequency on the dynamic characteristics of the beams are studied and described in detail. The numerical results show that the effects of the axial force and the moving velocity on the dynamic response of the beams are governed by the excitation frequency. The influence of acceleration, partial support by the elastic foundation and the significance of the second foundation parameter are also examined and highlighted.

1 Introduction

The analysis of beams on elastic foundation is one of important topics in civil engineering, and it was a subject of investigation for many decades. In his classical work, Hetényi (1946) has presented a number of solutions for finite and infinite beams resting on various types of elastic foundation, including the Winkler foundation, variable stiffness and continuum foundations, under static loads. To take care of the shortcomings of the Winkler foundation model, Hetényi himself proposed a foundation model in which the interaction among discrete Winkler springs is accomplished by incorporating an elastic beam or elastic plate, and the investigation on the beams resting on the Hetényi foundation was also described.

It is well known that the mechanical characteristics such as the displacement and the stress of a structure subjected to moving loads are quite different from those obtained by a static analysis of the structure subjected to the same loads. The displacement and the stress of the structure in a dynamic analysis depend not only on the magnitude of external loads, but also on the velocity and frequency of the loads.

The dynamic analysis of beams under moving loads plays an important role in the field of railway and bridge engineering, and this topic has attracted much attention from researchers for many years. The early work on the topic has been described by Timoshenko et al. (1974), where the governing equation for a uniform Bernoulli beam subjected to a moving harmonic force with constant velocity was solved by the mode superposition method. Fryba (1972) presented a solution for the vibrations of a simply supported beam under moving loads and axial forces. Employing the traditional plane Bernoulli beam element, Thambiratnam and Zhuge (1996) performed a dynamic analysis of beams resting on a Winkler elastic foundation subjected to moving loads by the finite element method. Chen et al. (2001) investigated the response of an infinite Timoshenko beam on a viscoelastic foundation to a moving harmonic load by deriving the dynamic stiffness matrix for the beam. The natural frequencies and mode shapes of Bernoulli-type beams subjected to moving loads with variable velocity have been investigated by Dugush and Eisengerger (2002) by both the modal and direct integration methods. Using the Fourier transform method, Kim (2004) obtained the steady-state response to moving loads of axial loaded beams resting on a Winkler elastic foundation. Adopting polynomials as trial function for the deflection in the Lagrangian equations, Kocatürk and Şimşek (2006) investigated the vibration of viscoelastic beams subjected to an eccentric compressive force and a moving harmonic force.

The objective of this paper is to investigate the dynamic response of prestressed Timoshenko beams resting on a two-parameter elastic foundation to a moving concentrated harmonic load by the finite element method. The

prestress is assumed to result from the initial loading by axial forces, and the variation of the moving velocity is also taken into consideration. Regarding the above cited references, two different features are included in the present work. Firstly, the shear deformation is introduced through a finite element formulation. Secondly, a two-parameter foundation model is adopted, which takes into account the interaction between springs of the traditional Winkler foundation through the introduction of a shear layer connecting the ends of Winkler springs to a beam. Different from the Hetényi foundation, the introduced shear layer in the two-parameter foundation model undergoes transverse shear deformations only, and this feature guarantees a simple mathematical form of the model, Dutta and Roy (2002). The accuracy and advantages of the two-parameter foundation in modelling the effect of elastic foundation support on structures has been investigated and described by Feng and Cook (1983).

Following this introduction, the paper is organized as follows. A beam element based on the field consistent approach for the dynamic analysis is formulated in Section 2. Section 3 describes the governing equations for the discrete beam under a moving load. The effects of prestress, foundation support, moving velocity as well as the excitation frequency on the dynamic response of the beams are numerically investigated in detail in Section 4. The main conclusions of the paper are summarized in Section 5.

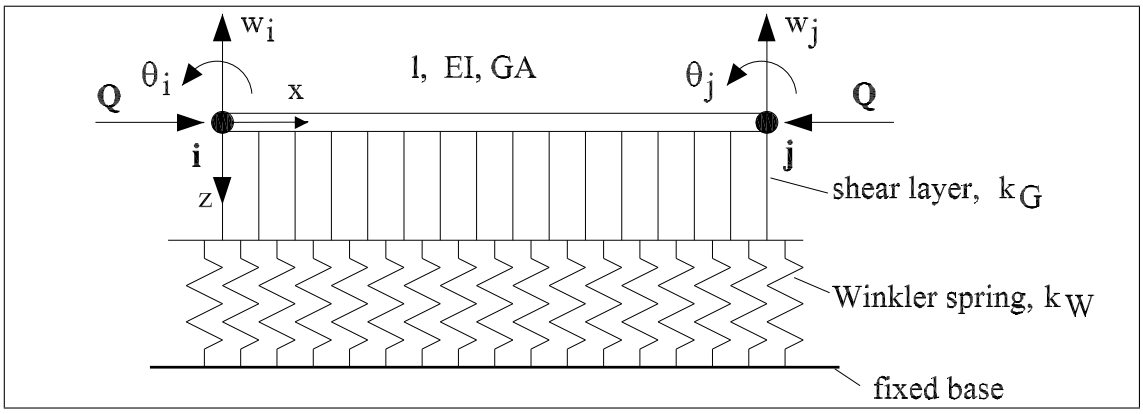

Figure 1. A two-node prestressed beam element resting on two-parameter foundation

2 Finite Element Formulation

Consider a two-node uniform beam element ij, resting on a two-parameter elastic foundation as shown in Figure 1. In the figure, l, A, I are the element length, cross-sectional area, and moment of inertia, respectively. The element is initially stressed by axial forces Q. At each node the element has two degrees of freedom, namely a lateral translation and a rotation about an axis normal to the plane (x, z). Thus, the vector of nodal displacements contains four components as

$$\mathbf{d} = \{w_i,\ \theta_i,\ w_j,\ \theta_j\}^{\mathrm{T}} \tag{1}$$

in which (and hereafter) the superscript $^{\mathrm{T}}$ refers to the transpose of a vector or a matrix.

In order to derive the stiffness and mass matrix for the finite element analysis we need to employ an interpolation scheme. Simple linear functions for both the lateral displacement w and rotation θ, as widely adopted in the field, Cook et al. (1989); Kien (2004), are possible. However, using such linear functions, the special technique should be adopted to prevent a possible shear locking problem. Recently, Luo (1998) demonstrated that a Timoshenko beam element formulated in the context of the so-called field consistent approach possesses many advantages, including the high accuracy and the absence of shear locking. The present work adopted this field consistent approach, and finds the interpolation functions by solving the homogenous equilibrium equations of a Timoshenko beam element

$$\begin{cases} EI\frac{\partial^2\theta}{\partial x^2} + \overline{GA}\left(\frac{\partial w}{\partial x} - \theta\right) & = 0 \\ \overline{GA}\left(\frac{\partial^2 w}{\partial x^2} - \frac{\partial\theta}{\partial x}\right) & = 0 \end{cases} \tag{2}$$

where EI and $\overline{GA}$ are the flexural and effective shear rigidities, respectively; $\overline{GA} = \psi GA$, with ψ is the correction factor, Shames and Dym (1985). Introducing a dimensionless parameter

$$\lambda = \frac{1}{l^2}\frac{EI}{\overline{GA}} \tag{3}$$

we can rewrite equation (2) in the form

$$\begin{cases} EI\frac{\partial^2\theta}{\partial x^2} + \frac{1}{\lambda l^2}EI\left(\frac{\partial w}{\partial x} - \theta\right) & = 0 \\ \frac{1}{\lambda l^2}EI\left(\frac{\partial^2 w}{\partial x^2} - \frac{\partial\theta}{\partial x}\right) & = 0 \end{cases} \tag{4}$$

Using the command `dsolve` in the symbolic software Maple (1991), we can easily obtain the general solutions for the system of equations (4) as

$$\begin{cases} w(x) = \frac{1}{6}C_1x^3 + \frac{1}{2}C_2x^2 + C_3x + C_4 \\ \theta(x) = C_1\lambda l^2 + \frac{1}{2}C_1x^2 + C_2x + C_3 \end{cases} \tag{5}$$

where the constant C_1, ..., C_4 are determined from element end conditions

$$\begin{cases} w_{|x=0} = w_i \quad ; \quad \theta_{|x=0} = \theta_i \\ w_{|x=l} = w_j \quad ; \quad \theta_{|x=l} = \theta_j \end{cases} \tag{6}$$

Expressing the displacement and the rotation in the forms

$$\begin{aligned} w(x) &= N_{w1}w_i + N_{w2}\theta_i + N_{w3}w_j + N_{w4}\theta_j = \mathbf{N}_w^{\mathrm{T}}\mathbf{d} \\ \theta(x) &= N_{\theta1}w_i + N_{\theta2}\theta_i + N_{\theta3}w_j + N_{\theta4}\theta_j = \mathbf{N}_\theta^{\mathrm{T}}\mathbf{d} \end{aligned} \tag{7}$$

where $\mathbf{N}_w = \{N_{w1},\ N_{w2},\ N_{w3},\ N_{w4}\}^{\mathrm{T}}$ and $\mathbf{N}_\theta = \{N_{\theta1},\ N_{\theta2},\ N_{\theta3},\ N_{\theta4}\}^{\mathrm{T}}$ are the vectors of interpolation functions for $w(x)$ and $\theta(x)$, respectively. From equations (5)-(7), we can obtain the expressions for N_{wi} and $N_{\theta i}$, $(i = 1..4)$. The detail of these expressions are given by equations (25) and (26) in the Appendix. It can be seen from equation (25) that in the limit as $\overline{GA} \to \infty$, the interpolation functions N_{wi} go back to the Hermitian polynomials which are employed in developing the traditional Bernoulli beam element, Cook et al. (1989). In this case, the element goes back to the traditional Bernoulli beam element, which has ability in modelling slender beams.

Having the interpolation functions derived, the stiffness and the consistent mass matrices for the beam element can be developed from strain energy and kinetic energy expressions. The strain energy of the element is stemming from the beam bending, the foundation deformation and the prestress due to the axial force Q

$$U = U_B + U_F + U_Q \tag{8}$$

in which the strain energy for a Timoshenko beam element with length of l is given by (Shames and Dym, 1985)

$$U_B = \frac{1}{2}\int_0^l \left[EI\left(\frac{\partial\theta}{\partial x}\right)^2 + \overline{GA}\left(\frac{\partial w}{\partial x} - \theta\right)^2\right] dx \tag{9}$$

The strain energy stored in the elastic foundation during the beam deformation is resulted from stretching of the Winkler springs and deformation of the shear layer as (Rao, 2003; Yokoyama, 1996)

$$U_F = \frac{1}{2}\int_0^l k_W w^2 dx + \frac{1}{2}\int_0^l k_G\left(\frac{\partial w}{\partial x}\right)^2 dx \tag{10}$$

where k_W is the Winkler foundation modulus, having units force per length^2 (N/m^2), and k_G with dimensions of force (N) is the stiffness of the shear layer. The geometric strain energy stemming from the prestressed effect of the axial force is given by (Géradin and Rixen, 1997)

$$U_Q = \frac{1}{2}\int_0^l Q\left(\frac{\partial w}{\partial x}\right)^2 dx \tag{11}$$

where Q (with units N) is positive in tension. From equations (7), (25) and (26) we can easily express the strain energy U defined by equation (8) in terms of the nodal displacements, e.g. the strain energy U_B has the form

$$\begin{aligned} U_B = \frac{2}{(1+12\lambda)^2 l^3}EI\Big\{ &\left[3(w_i - w_j)^2 + 3l(w_i - w_j)(\theta_i + \theta_j) + l^2(\theta_i^2 + \theta_i\theta_j + \theta_j^2)\right. \\ &\left. + 6\lambda l^2(1+6\lambda)(\theta_i - \theta_j)^2\right] + 9\lambda\left[2(w_i - w_j) + l(\theta_i + \theta_j)\right]^2\Big\} \end{aligned} \tag{12}$$

The expressions similar to equation (12) for U_F and U_Q can also easily be obtained. Finally, we can compute the element stiffness matrix as a summation of the stiffness matrices due to the beam bending, the foundation deformation and the prestress as

$$\mathbf{k} = \mathbf{k}_B + \mathbf{k}_F + \mathbf{k}_Q \tag{13}$$

where

$$\mathbf{k}_B = \frac{\partial^2 U_B}{\partial \mathbf{d}^2} \quad ; \quad \mathbf{k}_F = \frac{\partial^2 U_F}{\partial \mathbf{d}^2} \quad ; \quad \mathbf{k}_Q = \frac{\partial^2 U_Q}{\partial \mathbf{d}^2} \tag{14}$$

The detail expressions for $\mathbf{k}_B$, $\mathbf{k}_F$ and $\mathbf{k}_Q$ are given by equations (27)-(31) in the Appendix. It is noted that when λ approaches to zero, the stiffness matrices $\mathbf{k}_B$ and $\mathbf{k}_Q$ deduce exactly to the stiffness matrix of the traditional Bernoulli beam element and the geometrical stiffness matrix, which employed the Hermitian polynomials as interpolation functions, Cook et al. (1989); Géradin and Rixen (1997).

The element consistent mass matrix for the dynamic analysis can be obtained from the kinetic energy using the same interpolation functions N_{wi} and $N_{\theta i}$ ($i = 1..4$) for the displacement field, equations (25)-(26). To this end, we start from the kinematic energy expression, which for the Timoshenko beam element of the present work has the form (Géradin and Rixen, 1997)

$$T = \frac{1}{2}\int_0^l \rho A \dot{w}^2 dx + \frac{1}{2}\int_0^l \rho I \dot{\theta}^2 dx \tag{15}$$

where ρ is the mass density, and $\dot{w} = \partial w/\partial t$, $\dot{\theta} = \partial \theta/\partial t$. Using equation (7), we can write the kinetic energy in the form

$$\begin{aligned} T &= \frac{1}{2}\dot{\mathbf{d}}^{\mathrm{T}} \int_0^l \rho A \mathbf{N}_w^{\mathrm{T}} \mathbf{N}_w dx \dot{\mathbf{d}} + \frac{1}{2}\dot{\mathbf{d}}^{\mathrm{T}} \int_0^l \rho I \mathbf{N}_\theta^{\mathrm{T}} \mathbf{N}_\theta dx \dot{\mathbf{d}} \\ &= \dot{\mathbf{d}}^{\mathrm{T}} \mathbf{m}_{\dot{w}} \dot{\mathbf{d}} + \dot{\mathbf{d}}^{\mathrm{T}} \mathbf{m}_{\dot{\theta}} \dot{\mathbf{d}} = \dot{\mathbf{d}}^{\mathrm{T}} \mathbf{m} \dot{\mathbf{d}} \end{aligned} \tag{16}$$

with

$$\mathbf{m} = \mathbf{m}_{\dot{w}} + \mathbf{m}_{\dot{\theta}} = \frac{1}{2}\int_0^l \rho A \mathbf{N}_w^{\mathrm{T}} \mathbf{N}_w dx + \frac{1}{2}\int_0^l \rho I \mathbf{N}_\theta^{\mathrm{T}} \mathbf{N}_\theta dx \tag{17}$$

is the consistent mass matrix of the element. The detail expression for $\mathbf{m}_{\dot{w}}$ and $\mathbf{m}_{\dot{\theta}}$ are given by equations (32) and (33) in the Appendix. Again, in the limit as $\lambda \to 0$ the mass matrix $\mathbf{m}_{\dot{w}}$ deduces exactly to the consistent mass matrix of the traditional Bernoulli beam element as presented by Géradin and Rixen (1997).

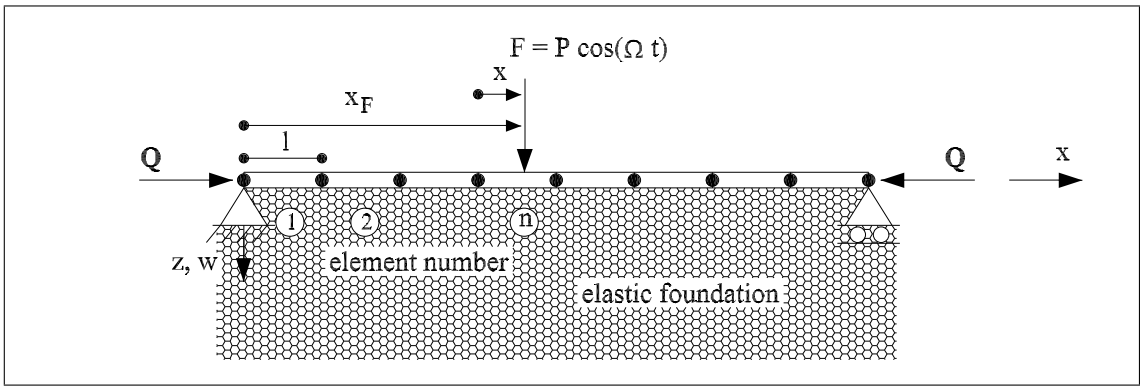

Figure 2. A prestressed beam resting on a two-parameter elastic foundation subjected to a moving harmonic load $F = P\cos(\Omega t)$.

3 Governing Equations

Consider a prestressed beam resting on the two-parameter foundation with a moving concentrated harmonic load, $F = P\cos(\Omega t)$, travelling along the beam from left to right as shown in Figure 2. In the figure, L is the total beam length, and x_F is the distance from the left end of the beam to the current moving load position. Assuming that at time $t = 0$ the load F is at the left-hand support and has a velocity of v_o, it then travels to the right, and at the right-hand support its velocity is v_f. Following the standard procedure of the finite element method, the beam is discretized into a number of finite elements. The equations of motion of the beam in terms of the finite element analysis when ignoring the damping effect can be written in the form (Cook et al., 1989)

$$\mathbf{M}\ddot{\mathbf{D}} + \mathbf{K}\mathbf{D} = P\cos(\Omega t)\mathbf{N} \tag{18}$$

where $\mathbf{M}$ and $\mathbf{K}$ are the structural mass and stiffness matrices, respectively. These matrices are obtained by assembling the element matrices $\mathbf{m}$ and $\mathbf{k}$ formulated in Section 2 in the standard way of the finite element method; $\mathbf{D}$ and $\ddot{\mathbf{D}} = \partial^2\mathbf{D}/\partial t^2$ are the vectors of structural nodal displacements and accelerations, respectively; $\mathbf{N}$ is the vector of shape functions for the beam, and having the form

$$\mathbf{N} = \{0,\ 0,\ 0,\ 0, ...\ N_{w1},\ N_{w2},\ N_{w3},\ N_{w4},\ 0,\ 0,\ 0,\ 0, ...\ 0,\ 0,\ 0,\ 0\}^{\mathrm{T}} \tag{19}$$

where N_{w1}, N_{w2}, N_{w3}, N_{w4} are defined by equation (25), in which the abscissa x is measured from the left-hand node of the current loading element to the position of the moving load, and for the case of equal-element mesh, this abscissa is calculated as

$$x = x_F - (n-1)l = \frac{v_f - v_o}{2\Delta t}t^2 + v_o t - (n-1)l \tag{20}$$

with l, as before, is the element length, and n denotes the number of the element on which the load is acting (see Figure 2); t is the current time, and Δt is the total time needed for the load to move completely from the left-hand support to the right-hand support.

The system of equation (18) is solved by the direct integration Newmark method using the average constant acceleration formula, which ensures an unconditional numerical stability, Géradin and Rixen (1997).

4 Numerical Investigations

Using the finite element formulated in Section 2 and the numerical algorithm described in Section 3, a computer code was developed and used in the dynamic analysis. To investigate the dynamic response, the beam with the following geometry and material data, previously employed by Kocatürk and Şimşek (2006), is adopted herewith

$L = 20$ m; $I = 0.08824$ m^4; $\rho A = 1000$ kg/m; $EI = 3 \times 10^9$ Nm^2, $\nu = 0.3$

where, in addition to the previous notations, ν denotes the Poisson ratio. The amplitude of the moving load is taken as $P = 100$ kN.

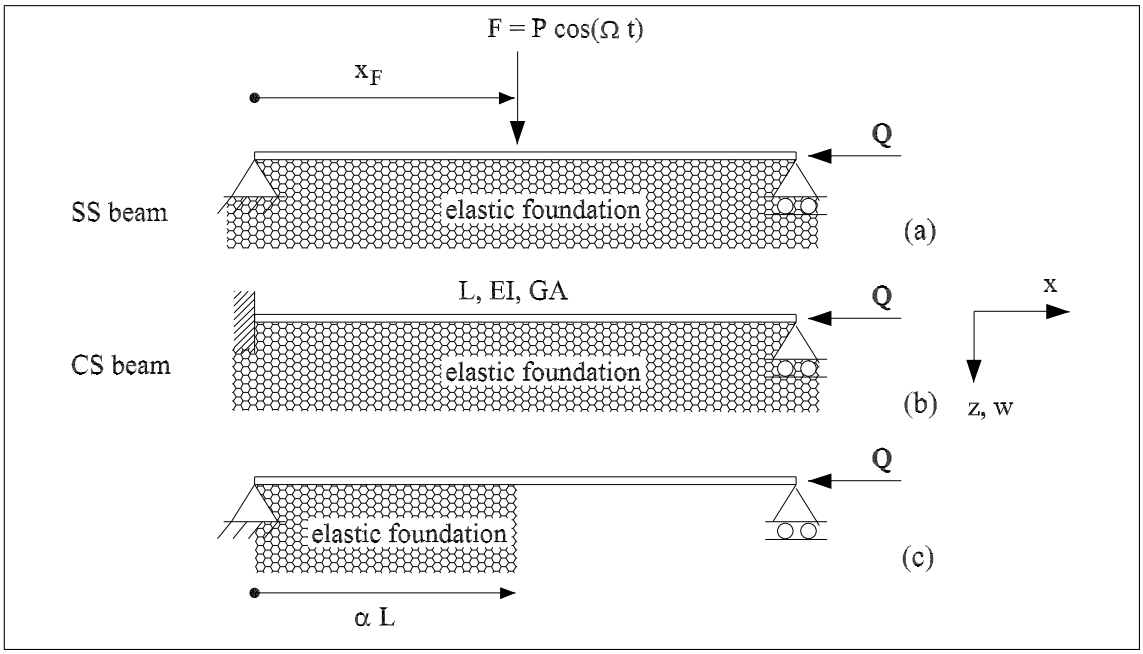

Figure 3. Beams for numerical investigation

Two types of boundary conditions, namely simply supported (SS) and clamped at one end and simply supported at the other (CS) as respectively shown in Figure 3(a) and Figure 3(b) are considered. The effect of partial support by the elastic foundation is examined by assuming that the beams are supported on a part αL, with $0 \leq \alpha < 1$, from the left-hand end as typically depicted in Figure 3(c) for the SS beam. For the convenience of discussion, α is called the supporting parameter.

The computation in this Section is performed with a mesh of 20 equal elements, and the correction factor ψ is taken by $\psi = \frac{10(1+\nu)}{(12+11\nu)}$.

(k_1, k_2)	r	μ	Naidu and Rao (1995)	(k_1, k_2)	r	μ	Naidu and Rao (1995)
(0,0)	0.0	3.1347	3.1415	(100,0.5)	0.0	3.9561	3.9608
	0.2	2.9646	2.9734		0.2	3.7415	3.7487
	0.4	2.7589	2.7705		0.4	3.4818	3.4928
	0.6	2.4930	2.5097		0.6	3.1462	3.1635
	0.8	2.0963	2.1257		0.8	2.6456	2.6782
(1,0)	0.0	3.1428	3.1496	(100,1)	0.0	4.1392	4.1437
	0.2	2.9723	2.9810		0.2	3.9146	3.9218
	0.4	2.7660	2.7776		0.4	3.6430	3.6541
	0.6	2.4994	2.5161		0.6	3.2918	3.3095
	0.8	2.1017	2.1312		0.8	2.7681	2.8014
(100,0)	0.0	3.7433	3.7483	(100,2.5)	0.0	4.5783	4.5824
	0.2	3.5402	3.5477		0.2	4.3299	4.3370
	0.4	3.2945	3.3055		0.4	4.0294	4.04.8
	0.6	2.9769	2.9940		0.6	3.6410	3.6594
	0.8	2.5033	2.5350		0.8	3.0617	3.0964

Table 1: Frequency parameter of the SS beam fully supported by the elastic foundation at various values of the compressive axial force and the foundation parameters

4.1 Model Verification

This subsection aims to verify the accuracy of the formulated element and the described numerical algorithm. To this end, the eigenfrequency and the dynamic response of the SS beam is computed and compared to the published ones. Following the work of Naidu and Rao (1995), we introduce herewith the dimensionless parameters k_1 and k_2 representing the stiffness of the Winkler springs and the shear layer of the foundation

$$k_1 = \frac{L^4}{EI} k_W \quad ; \quad k_2 = \frac{L^2}{\pi^2 EI} k_G \tag{21}$$

and a dimensionless parameter representing the axial force

$$f = \frac{L^2}{EI} Q \tag{22}$$

Furthermore, we also introduce the frequency parameter defined as

$$\mu = \left(\frac{\rho A L^4}{EI} \omega_1^2 \right)^{1/4} \tag{23}$$

with ω_1 (rad/s) is the fundamental frequency (the first natural frequency) of the beams.

Table 4.1 lists the frequency parameter of the SS beam fully supported by the elastic foundation at various values of the compressive axial force and the foundation parameters. In the table, $r = f/f_b$ is the ratio of the axial load parameter f, defined by equation (22), and the buckling load parameter f_b corresponding to the Euler buckling load Q_b, which can be obtained by solving the eigenvalue problem

$$\left(\mathbf{K}_B + \mathbf{K}_F - Q_b \mathbf{K}_Q \right) \mathbf{D} = \mathbf{0} \tag{24}$$

where $\mathbf{K}_B$, $\mathbf{K}_F$ and $\mathbf{K}_Q$ are the structural stiffness matrices, obtained by assembling the previous formulated element matrices $\mathbf{k}_B$, $\mathbf{k}_F$, $\mathbf{k}_Q$ in the standard way of the finite element method, respectively. It is noted that by writing the eigenvalue problem in the form (24), the axial force Q should be omitted from $\mathbf{K}_Q$.

It is seen from Table 4.1 that regardless of the axial force and the foundation stiffness, the frequency parameter of the SS beam fully resting on the elastic foundation obtained in the present work is in good agreement with that reported by Naidu and Rao (1995), who computed the frequency parameter by using the traditional Bernoulli beam elements. It is necessary to note that the beam with the above geometry data is quite slender, so that the frequencies are hardly affected by the shear deformation.

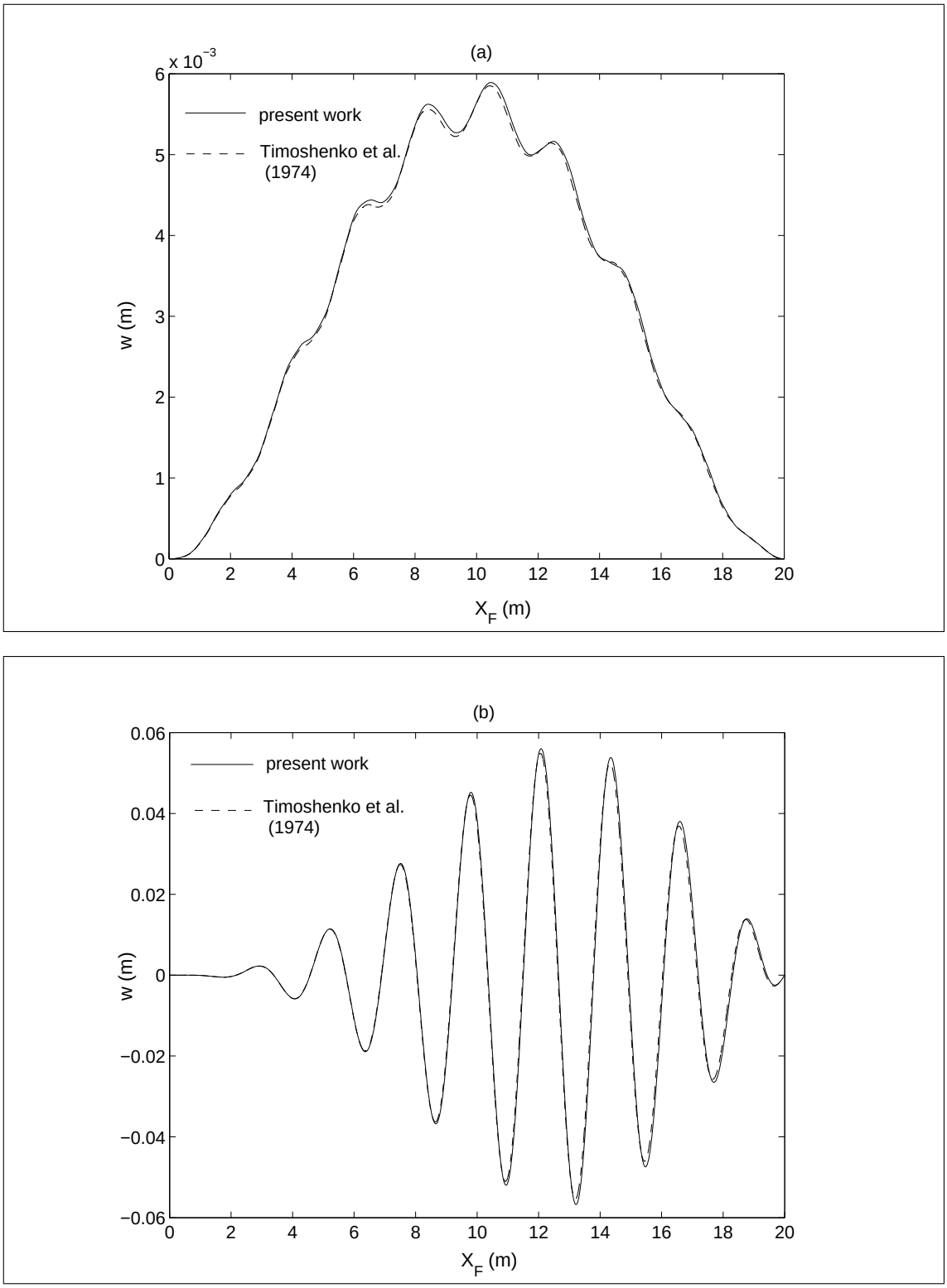

Figure 4. Deflection under a moving load of the SS beam without foundation support and axial force for the case of a constant velocity $v = 15$ m/s and with different excitation frequencies: (a) $\Omega = 0$ rad/s, (b) $\Omega = 40$ rad/s.

Figure 4 shows the deflection of the SS beam without the foundation support and the axial force under a constant speed moving load and with the excitation frequency of 0 and 40 rad/s. For the purpose of calibration, the analytical solution presented by Timoshenko et al. (1974) is also depicted in the figure. The deflections in the figure here and afterwards are computed at the load point. As seen from Figure 4, the deflections obtained by the numerical method in the present work are in excellent agrement with the results using the mode superposition method by Timoshenko et al. (1974) in the case of the moving load ($\Omega = 0$), and in the case of the moving harmonic load ($\Omega = 40$ rad/s). It is noted that the excitation frequency $\Omega = 40$ rad/s employed in the analysis is very near the

fundamental frequency of the SS beam ($\omega_1 = 42.5509$ rad/s, see Table 4.1), so that the deflection of the beam shown in Figure 4(b) is much larger than that of Figure 4(a) due to the resonance effect. The numerical results show the accuracy of the formulated element and the numerical algorithm in computing the dynamic response of the beam.

4.2 Effect of compressive axial force

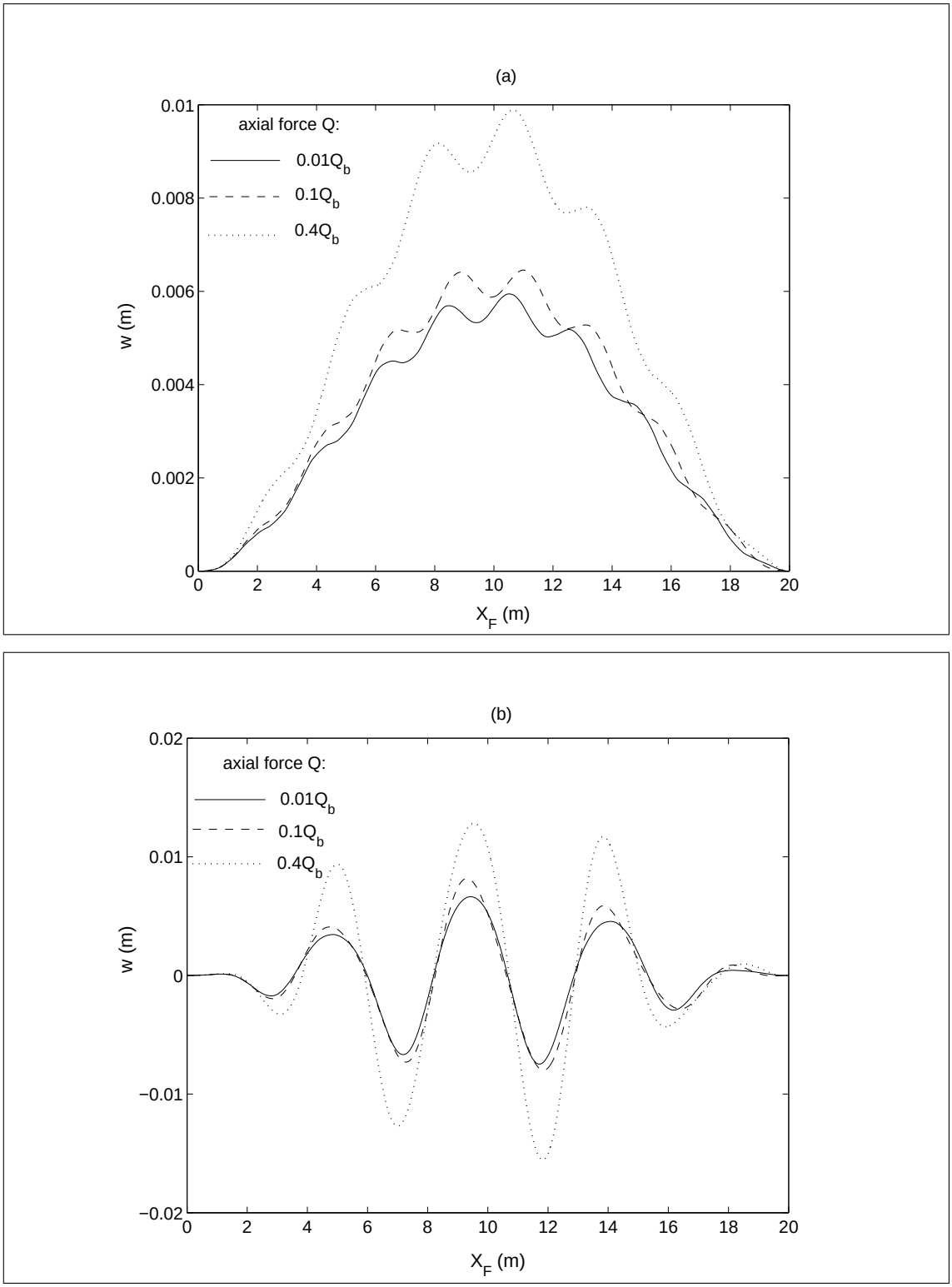

Figure 5. Effect of compressive axial force on the dynamic response of the SS beam without foundation support for the case of constant velocity $v = 15$ m/s and different excitation frequencies: (a) $\Omega = 0$ rad/s, (b) $\Omega = 20$ rad/s.

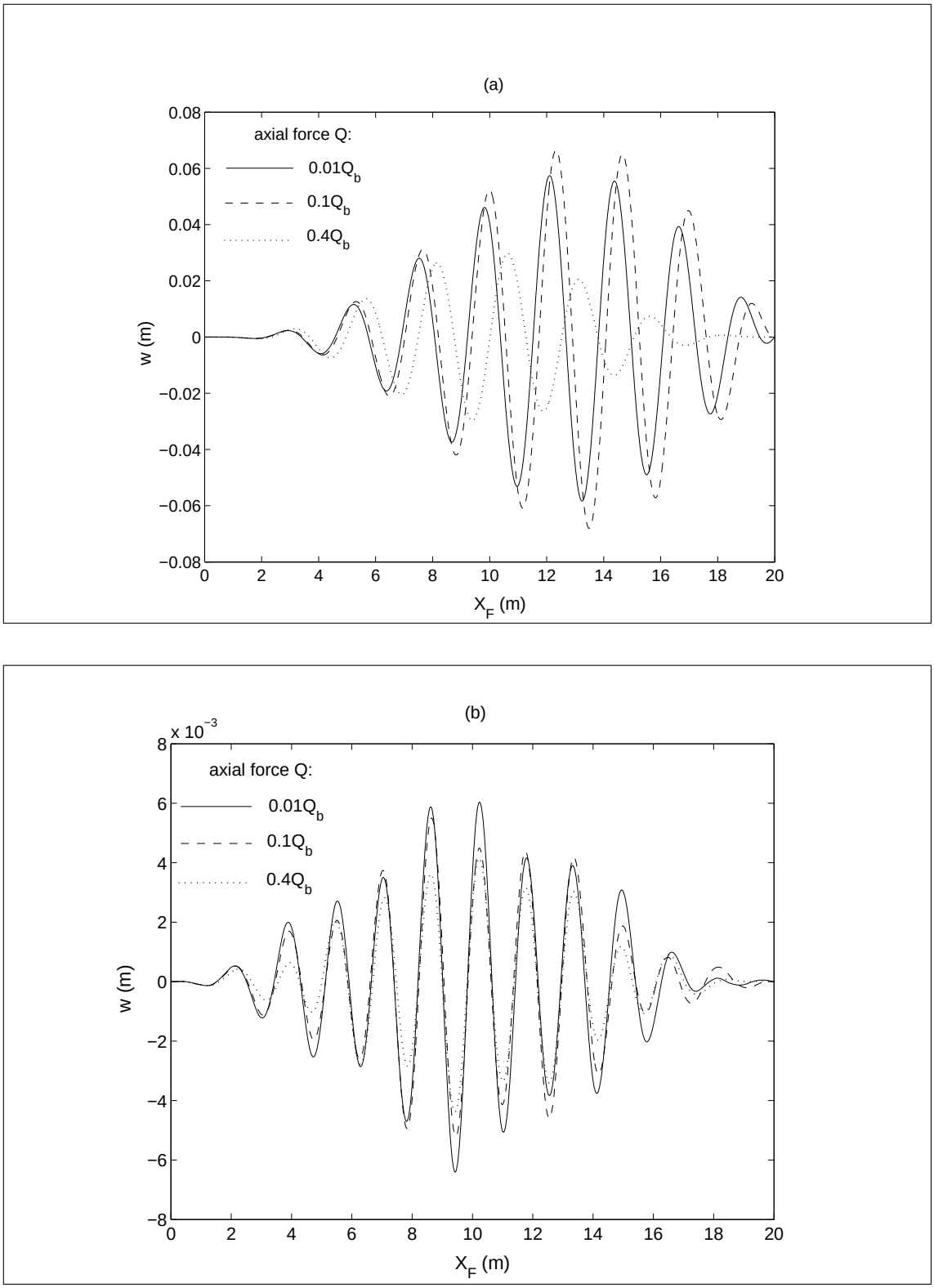

Figure 6. Effect of compressive axial force on the dynamic response of the SS beam without foundation support for the case of constant velocity $v = 15$ m/s and different excitation frequencies: (a) $\Omega = 40$ rad/s, (b) $\Omega = 60$ rad/s.

The effect of the compressive axial force on the dynamic response of the SS beam without foundation support for the case of constant velocity $v = 15$ m/s and different excitation frequencies is depicted in Figure 5 and Figure 6. In the figures, Q_b, as mentioned above is the Euler buckling load of the beam. As seen from the figures, the effect of the axial force depends on the the excitation frequencies, and with the excitation frequencies are considerably below the fundamental frequency or zero, the dynamic deflection of the beam is larger for a higher compressive axial force (see Figure 5). This numerical result is in agreement with the static analysis, in which the compressive

axial force reduces the bending stiffness of beams, Ghali and Neville (1995). When the excitation frequency is relatively higher than the fundamental frequency, the influence of the axial force on the dynamic response, as seen from Figure 6(b), is opposite: the dynamic deflection of the beam is smaller at a higher compressive axial force. With the excitation frequencies near the fundamental frequency (Figure 6(a)), the situation is mixed, the deflection firstly increases with an increment in the axial force, it then decreases.

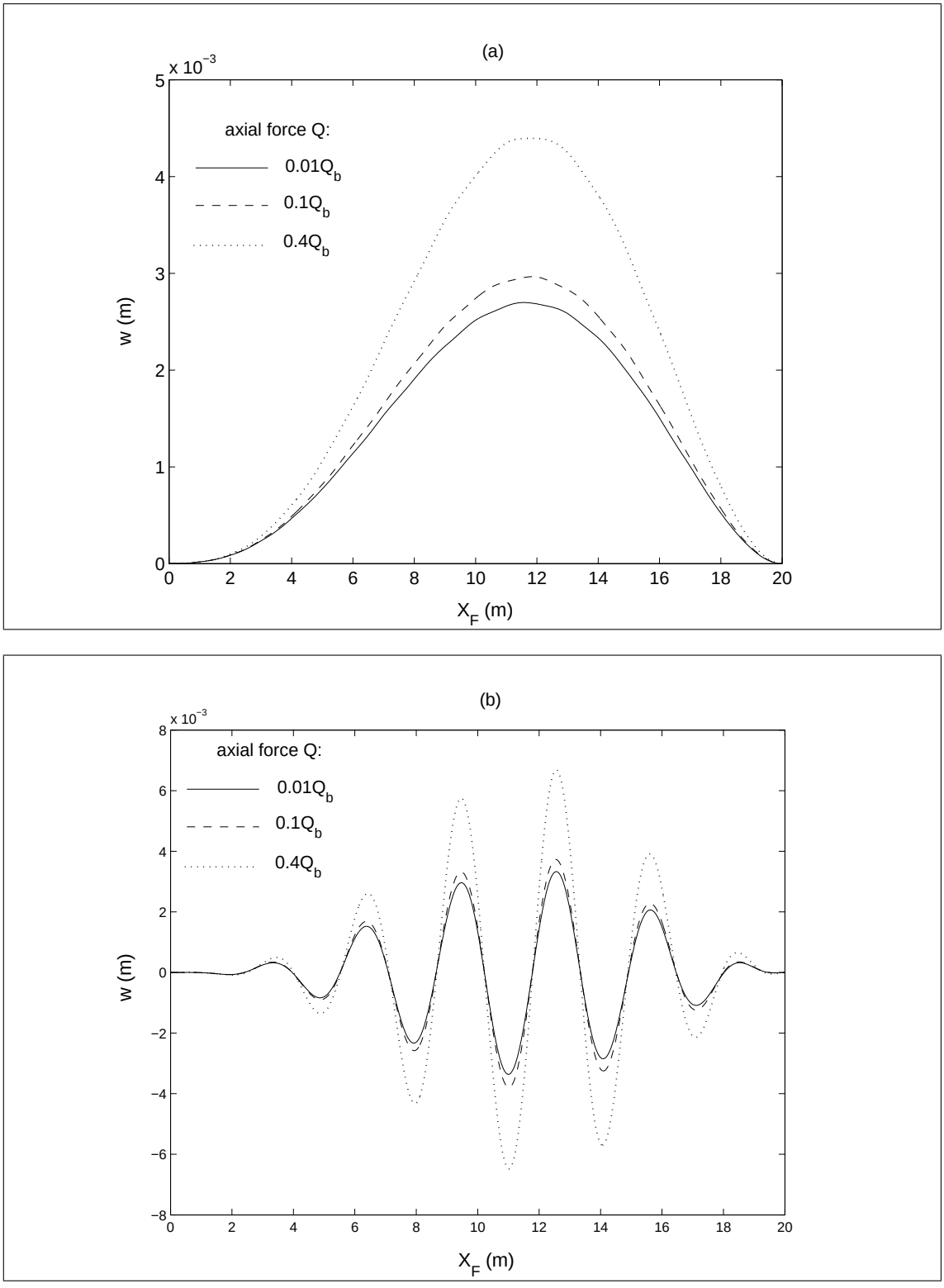

Figure 7. Effect of compressive axial force on the dynamic response of the CS beam without foundation support for the case of constant velocity $v = 15$ m/s and different excitation frequencies: (a) $\Omega = 0$ rad/s, (b) $\Omega = 30$ rad/s.

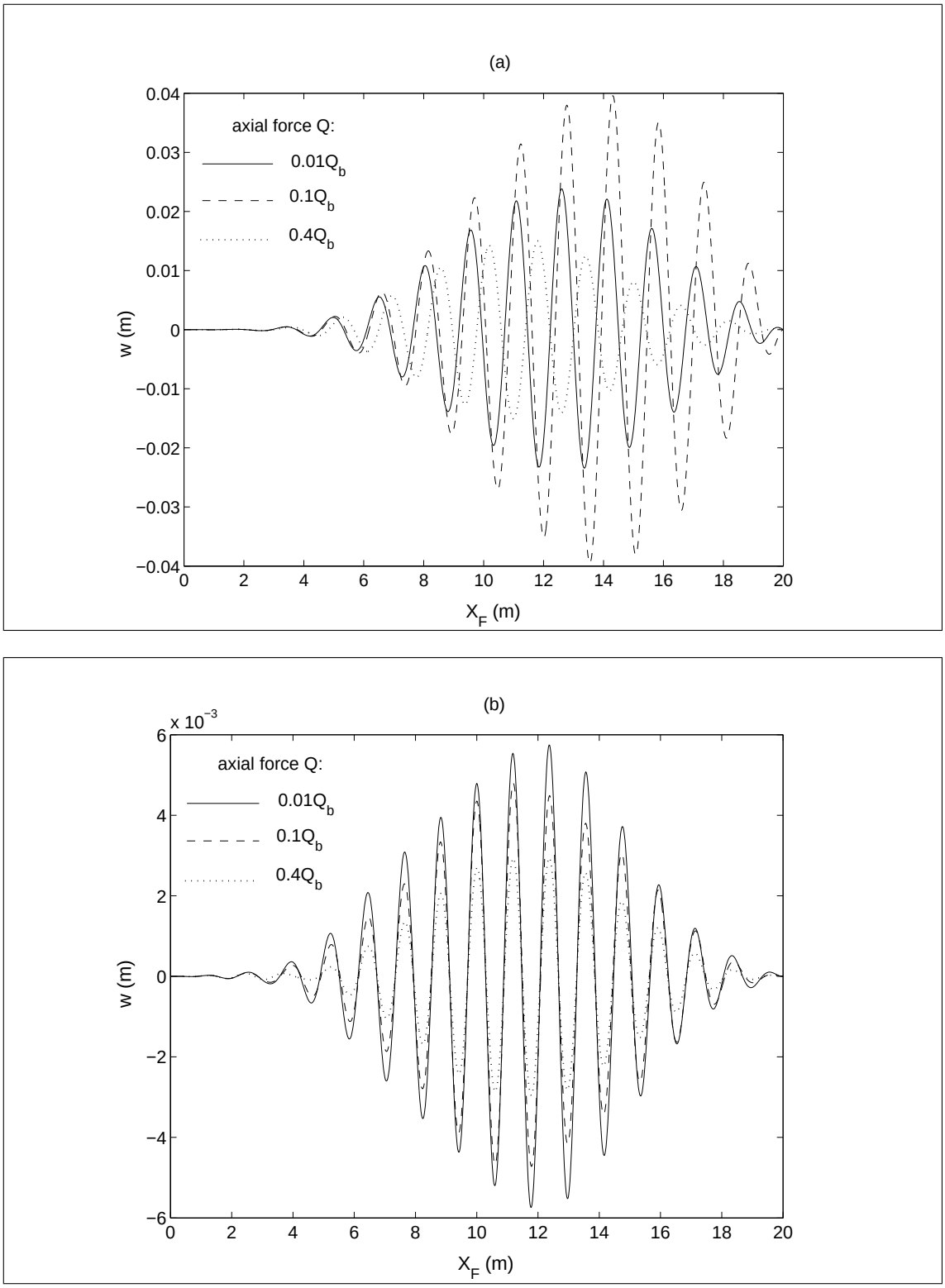

Figure 8. Effect of compressive axial force on the dynamic response of the CS beam without foundation support for the case of constant velocity $v = 15$ m/s and different excitation frequencies: (a) $\Omega = 60$ rad/s, (b) $\Omega = 80$ rad/s.

The above remark on the effect of the axial force, as seen from Figure 7 and Figure 8, is the same for the CS beam. It is noted that the effect of the axial force obtained in the present work is different from that reported by Kocatürk and Şimşek (2006), who concluded that this effect is very small and can be ignored. The reason of this difference may be of that the largest axial force employed by Kocatürk and Şimşek is too small, just less than 3% of the buckling load, and the effect is hardly recognized.

The effect of the compressive axial force on the dynamic response of the SS and CS beams resting on the two-

parameter foundation is depicted in Figure 9 and Figure 10, respectively. The numerical results shown in the figures are obtained with $k_1 = 100$ and $k_2 = 1$, and in this case the fundamental frequency of the SS and CS beams is 74.1899 rad/s and 91.2939 rad/s, respectively (see Table 4.1 for the SS beam. The natural frequency of the CS beam is not shown herein). The effect is almost the same as that of the case without the foundation support. In addition to the higher frequency, the deflections of the beams with the foundation support are much lower since the structures become much stiffer with the presence of the foundation.

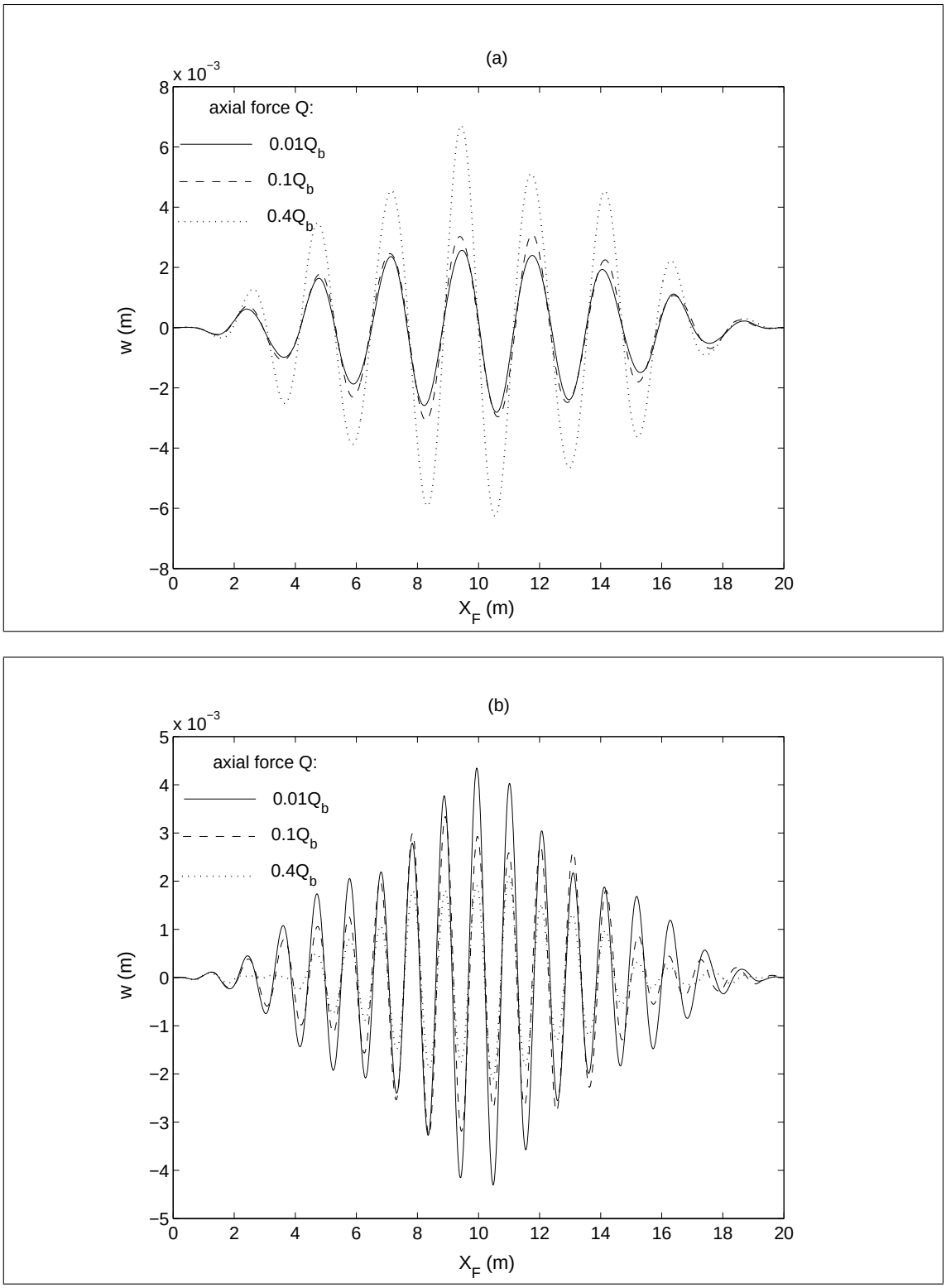

Figure 9. Effect of compressive axial force on the dynamic response of the SS beam resting on the two-parameter elastic foundation for the case of constant velocity $v = 15$ m/s and different excitation frequencies: (a) $\Omega = 40$ rad/s, (b) $\Omega = 90$ rad/s ($k_1 = 100$, $k_2 = 1$).

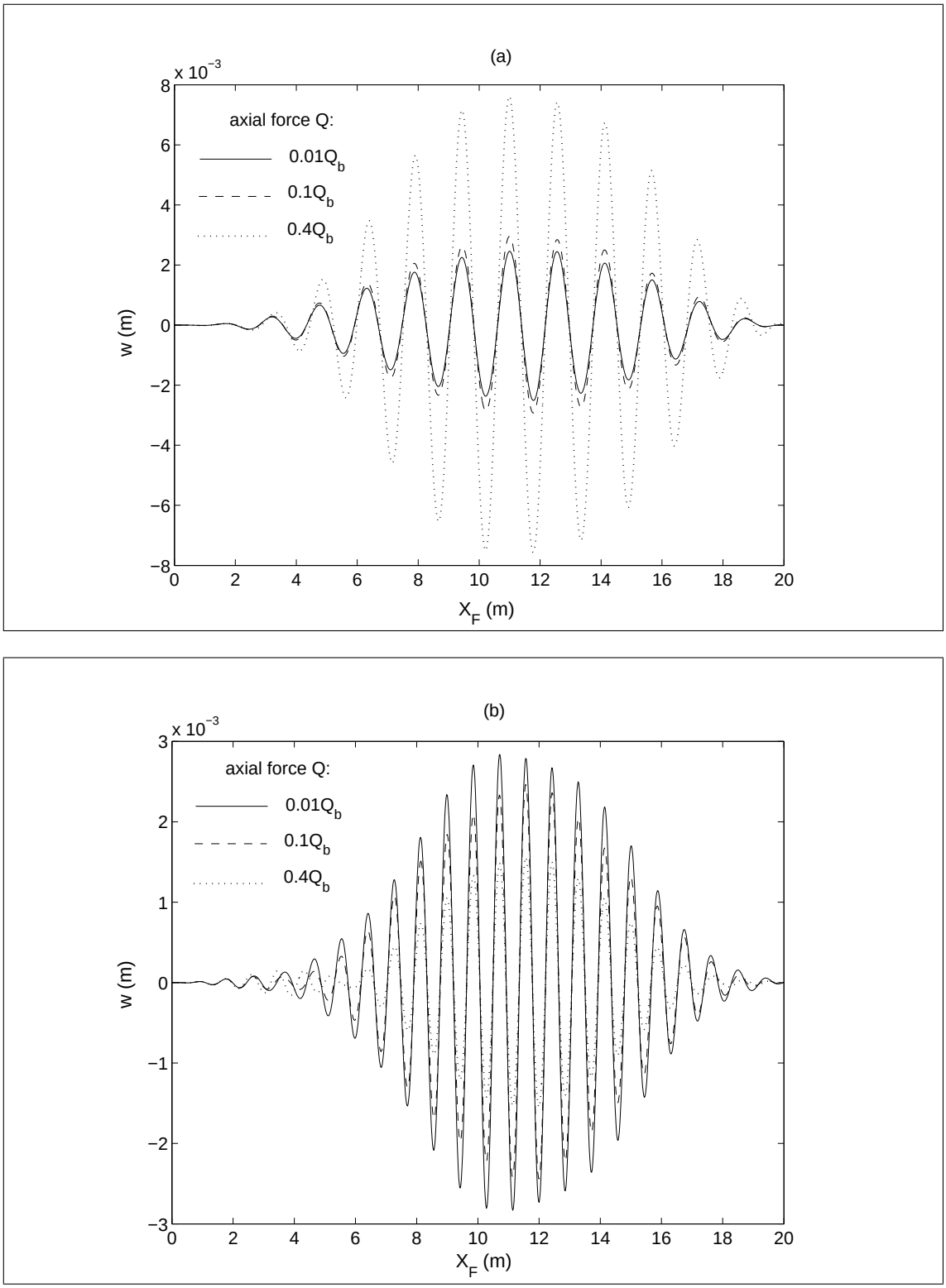

Figure 10. Effect of compressive axial force on the dynamic response of the CS beam resting on the two-parameter elastic foundation for the case of constant velocity $v = 15$ m/s and different excitation frequencies: (a) $\Omega = 60$ rad/s, (b) $\Omega = 110$ rad/s ($k_1 = 100$, $k_2 = 1$).

4.3 Effect of moving velocity and acceleration

To investigate the effect of the moving velocity on the dynamic response of the beams, the axial force and the foundation stiffness are kept to be constant, namely $Q = 0.2Q_b$ and $(k_1, k_2) = (100, 1)$. The fundamental frequency of the beams in this case is 66.3570 rad/s for the SS beam, and 82.0219 rad/s for the CS beam. The computation is performed with various values of the constant velocity, v = 20, 40, 60, 100 m/s, and with excitation

frequencies near and far from the fundamental frequencies.

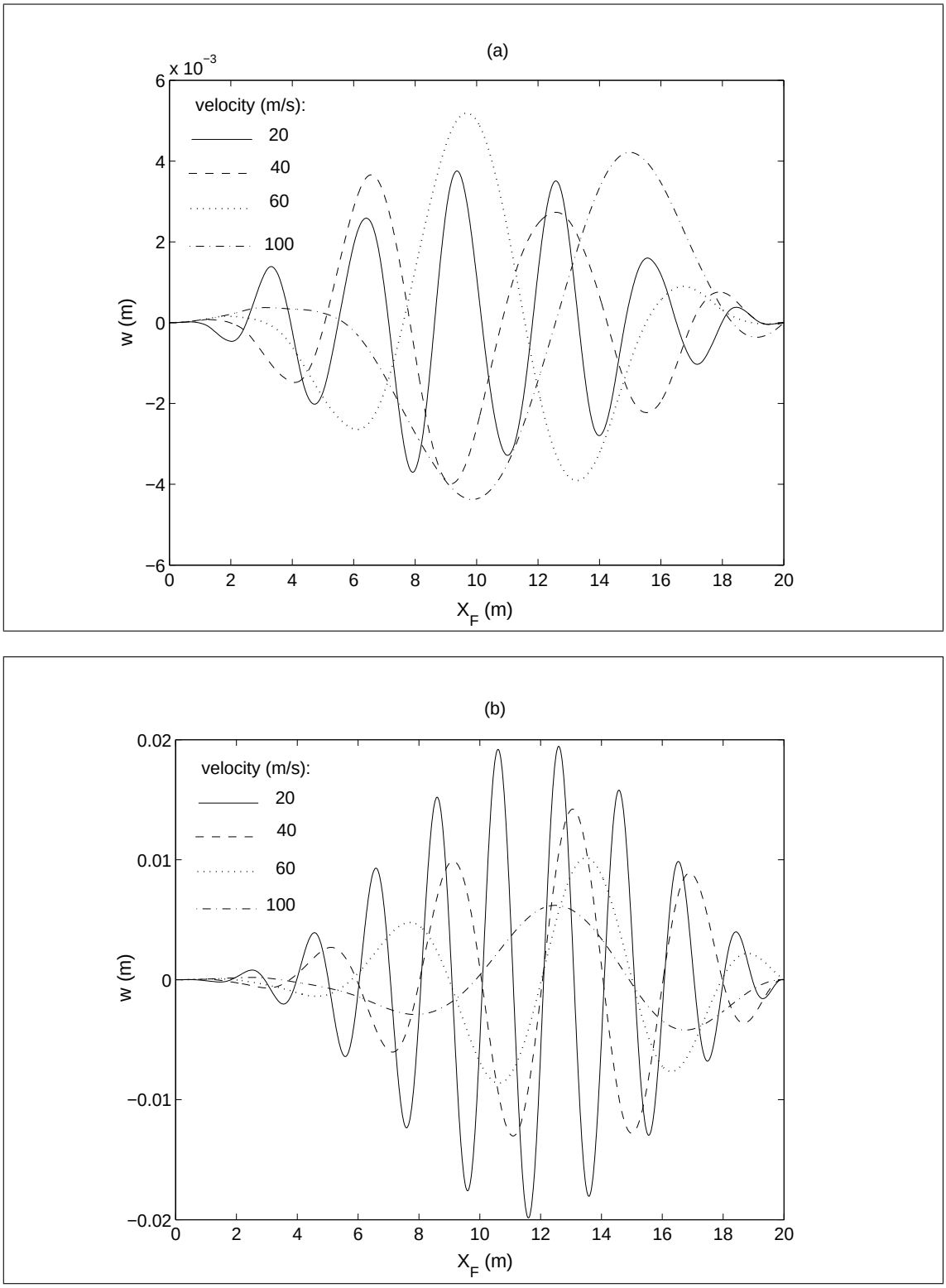

Figure 11. Effect of moving velocity on the dynamic response of the prestressed SS beam resting on the two-parameter elastic foundation with different excitation frequencies: (a) $\Omega = 40$ rad/s, (b) $\Omega = 60$ rad/s ($Q = 0.2Q_b$, $k_1 = 100$, $k_2 = 1$).

Figure 11 shows the effect of the moving velocity on the dynamic response of the prestressed SS beam resting on the two-parameter elastic foundation. The corresponding effect for the CS beam is depicted in Figure 12. Again, the effect of the moving velocity on the dynamic response is governed by the excitation frequencies. For the excitation frequency well below the fundamental frequencies, the dynamic deflection of the beams firstly increases with an increment in the moving velocity, it then decreases, regardless of the boundary conditions (Figure 11(a)

and Figure 12(a)). In other words, at a given axial force and foundation stiffness, there is a critical velocity at which the dynamic deflection reaches a maximum value for the case of excitation frequencies much different from the fundamental frequencies. On the contrary, the deflections of the beams are gradually decreased in raising the velocity when the excitation frequencies are near the fundamental frequencies (Figures 11(b) and 12(b)).

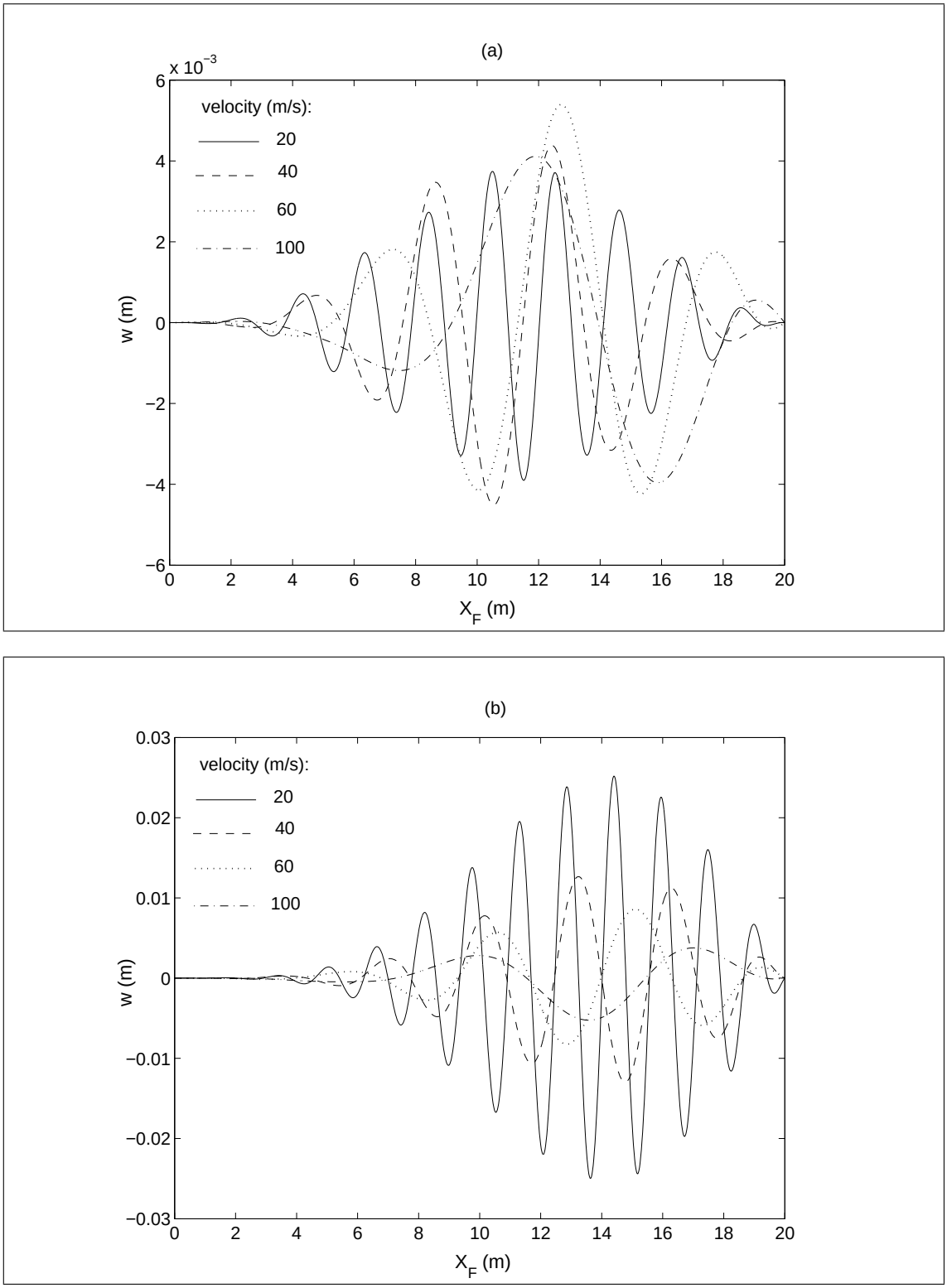

Figure 12. Effect of moving velocity on the dynamic response of the prestressed CS beam resting on the two-parameter elastic foundation with different excitation frequencies: (a) $\Omega = 60$ rad/s, (b) $\Omega = 80$ rad/s ($Q = 0.2Q_b$, $k_1 = 100$, $k_2 = 1$).

The acceleration of the moving load can be defined by the difference between the velocity of the moving load at the left-hand and right-hand ends of the beams, v_o and v_f, and in order to examine the effect of the accelerated

phenomenon, in addition to the above-mentioned parameters relating the axial force and the foundation stiffness, the moving velocity at the left-hand end of the beams is kept to be constant $v_o = 15$ m/s, and the computation is performed with different values of v_f, namely 20, 30, 40 and 50 m/s.

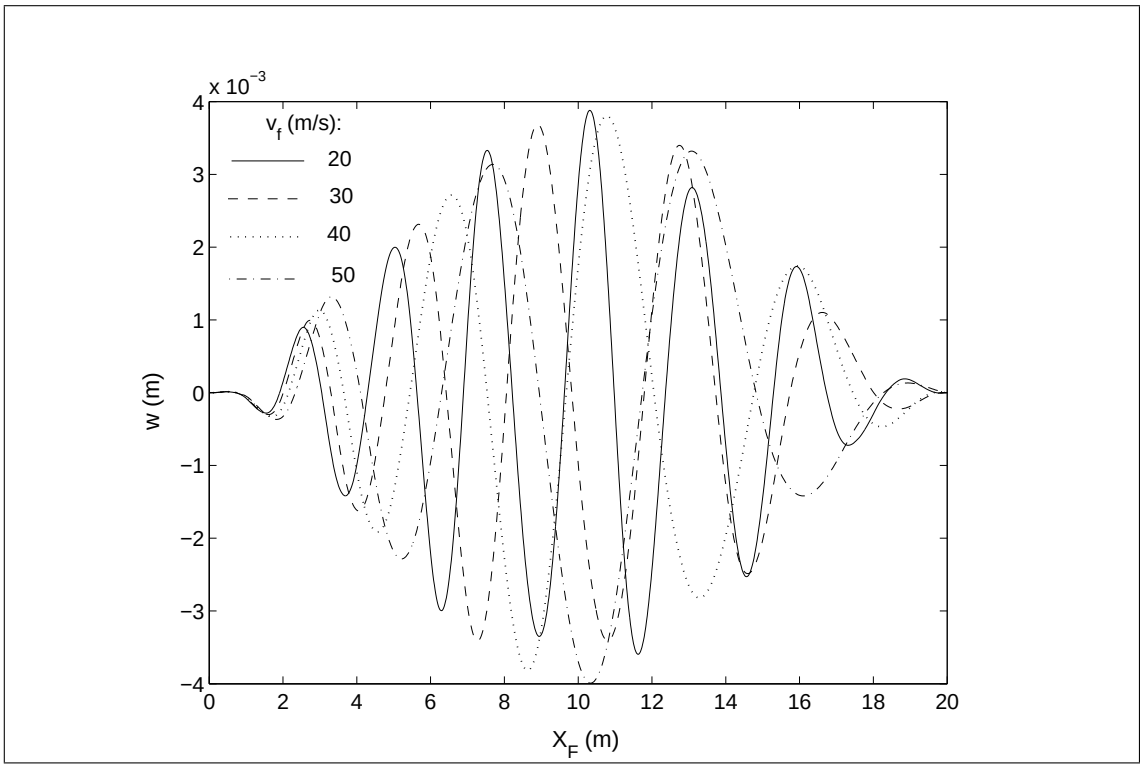

Figure 13. Effect of acceleration on the dynamic response of the prestressed SS beam resting on the two-parameter elastic foundation with an excitation frequency $\Omega = 40$ rad/s ($v_o = 15$ m/s, $Q = 0.2Q_b$, $k_1 = 100$, $k_2 = 1$).

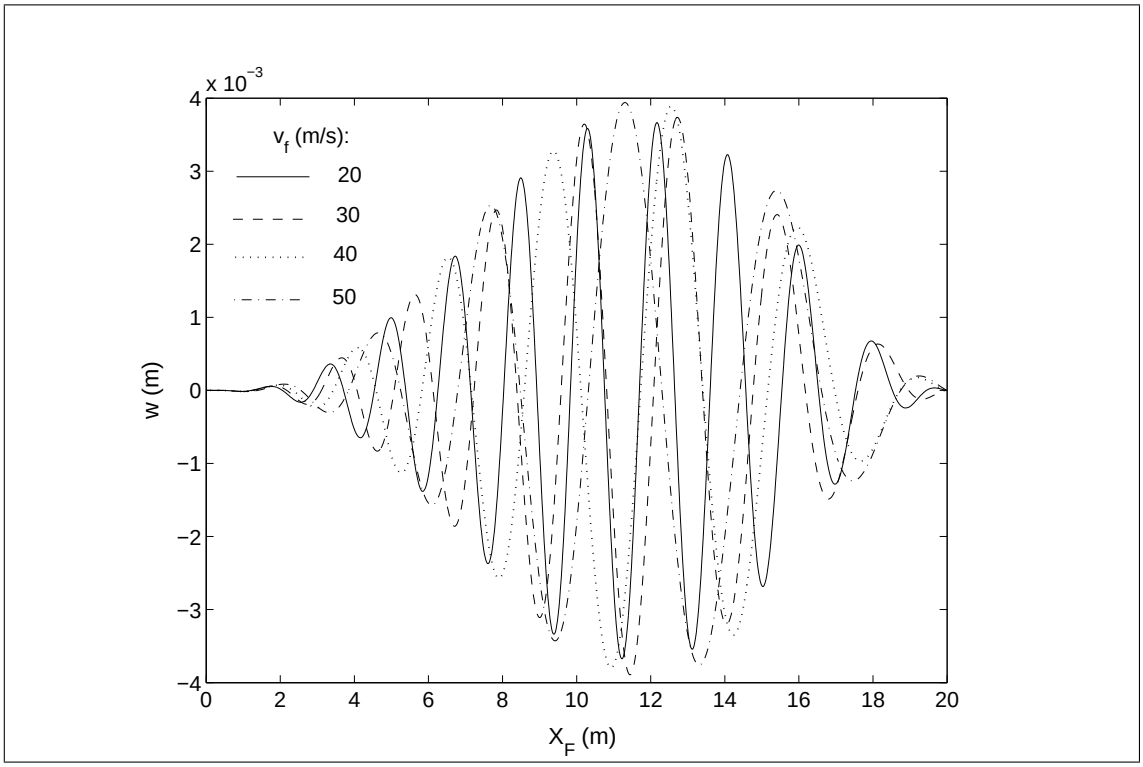

Figure 14. Effect of acceleration on the dynamic response of the prestressed CS beam resting on the two-parameter elastic foundation with an excitation frequency $\Omega = 60$ rad/s ($v_o = 15$ m/s, $Q = 0.2Q_b$, $k_1 = 100$, $k_2 = 1$).

Figures 13 and 14 show the effect of the acceleration on the dynamic response of the SS and CS beams, respectively. The curves in the figures are obtained for the excitation frequencies well below the fundamental frequencies. As seen from the figures, the dynamic response of the beams is somehow affected by the acceleration. At the given axial force, the foundation stiffness and the excitation frequency, the maximum dynamic deflection increases with an increment in the acceleration, it then reaches a maximum value.

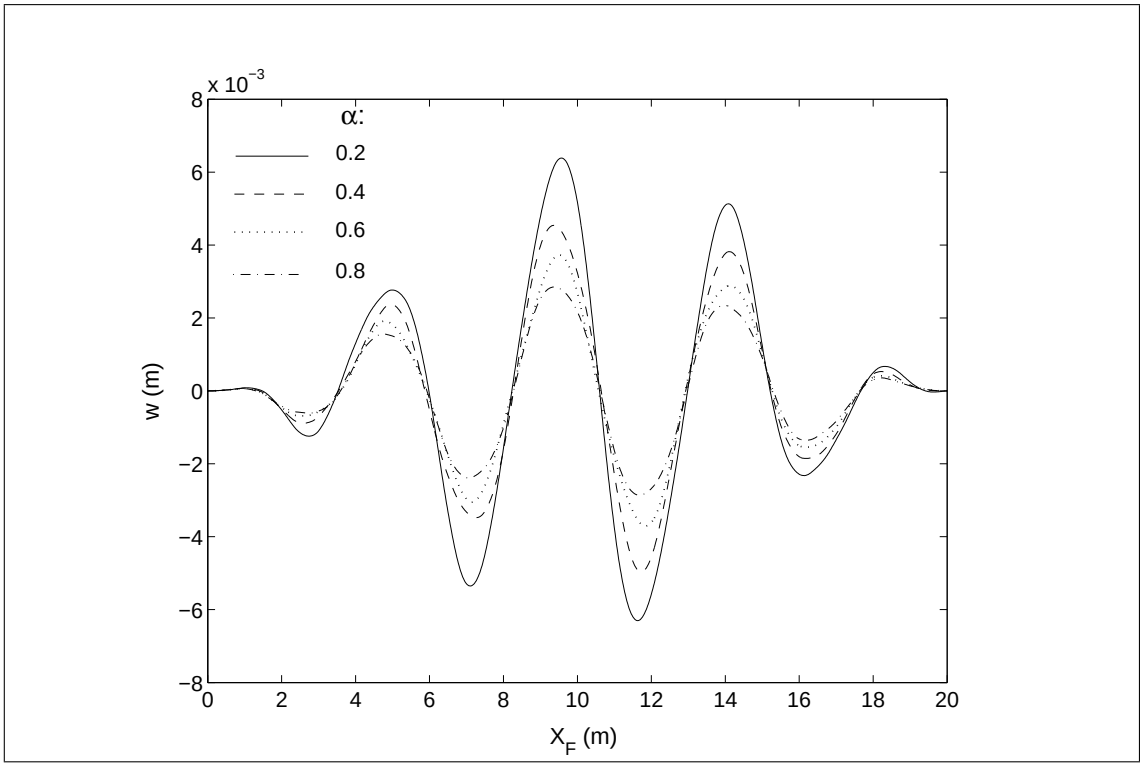

Figure 15. Effect of partial support by the elastic foundation on the dynamic response of the prestressed SS beam to the moving load ($v = 15$ m/s, $\Omega = 20$ rad/s, $Q = 0.2Q_b$, $k_1 = 100$ and$k_2 = 1$).

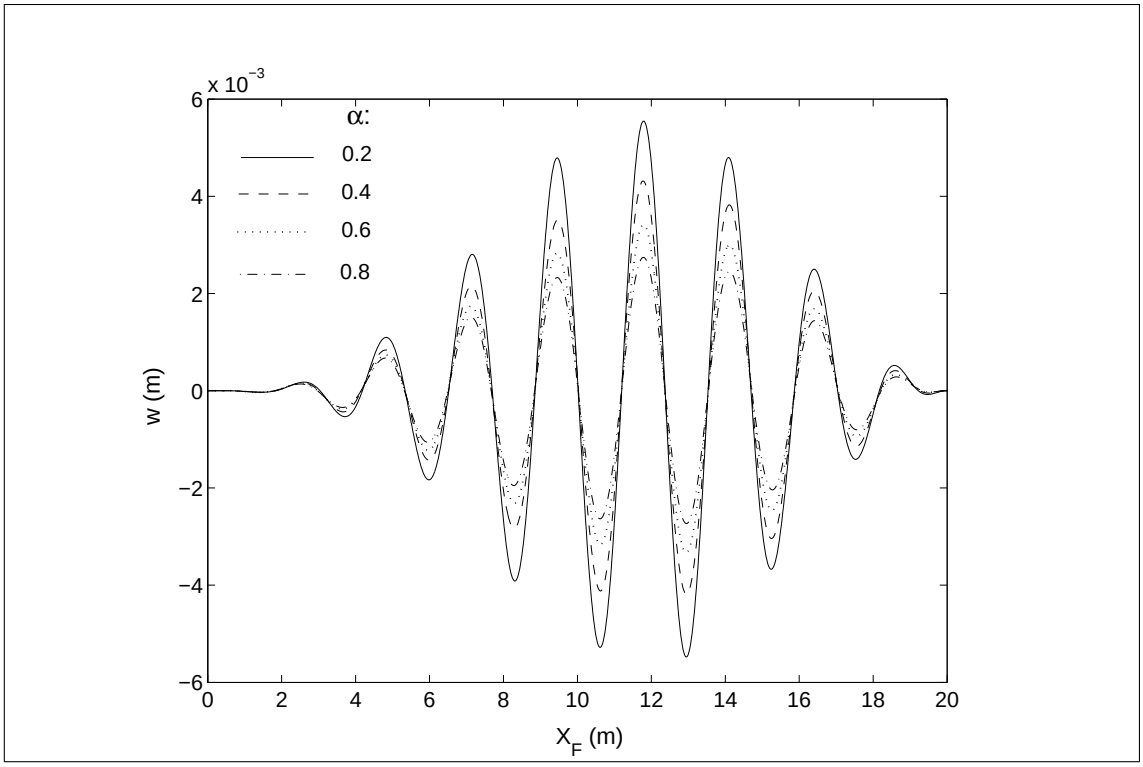

Figure 16. Effect of partial support by the elastic foundation on the dynamic response of the prestressed CS beam to the moving load ($v = 15$ m/s, $\Omega = 40$ rad/s, $Q = 0.2Q_b$, $k_1 = 100$ and $k_2 = 1$).

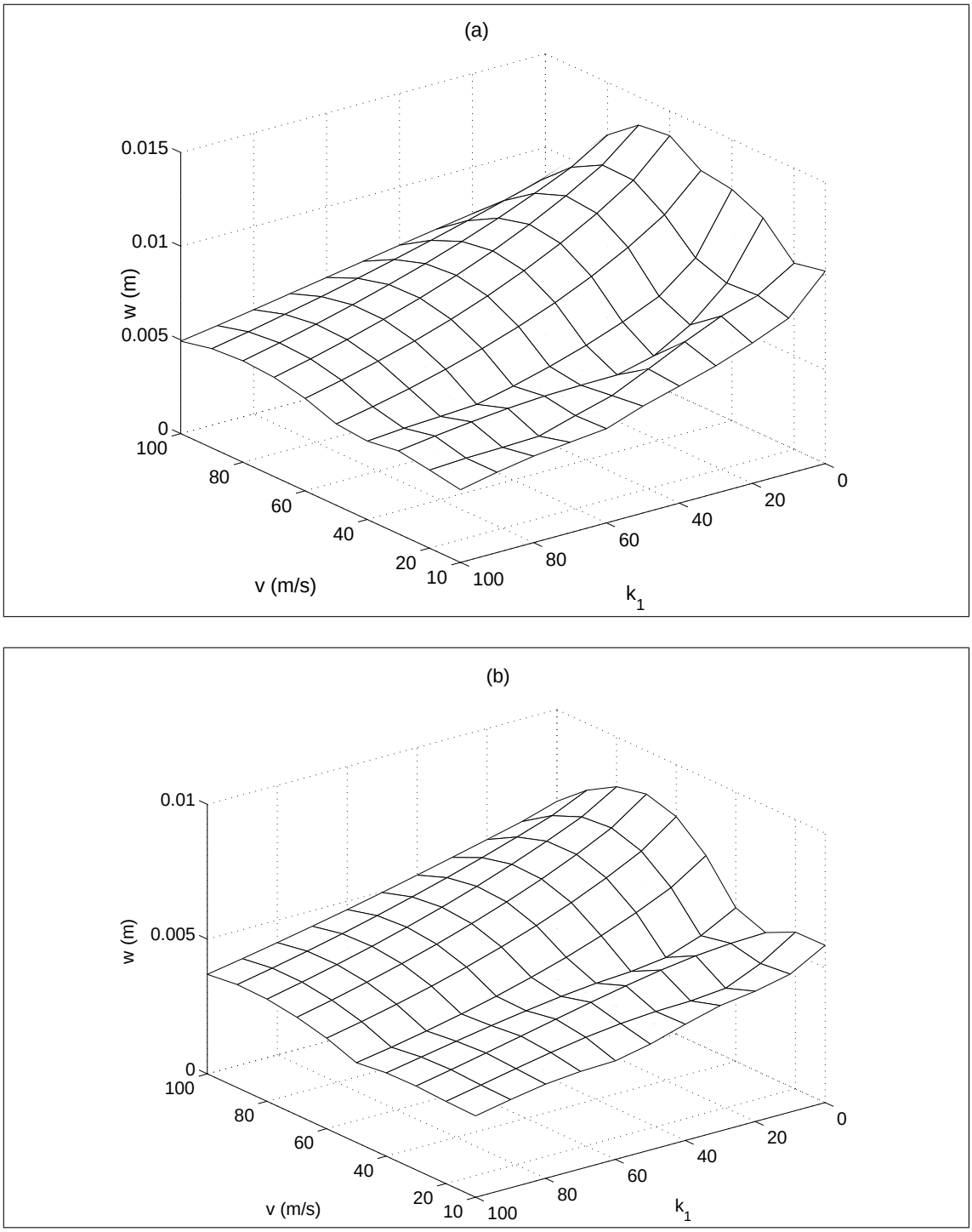

Figure 17. Moving velocity and foundation stiffness versus the maximum dynamic deflection of the prestress SS beam with an excitation frequency $\Omega = 20$ rad/s and different values of second foundation parameter: (a) $k_2 = 0$, (b) $k_2 = 0.5$, ($Q = 0.2Q_b$).

4.4 Effect of partial support

The effect of the partial support by the elastic foundation on the dynamic response of the prestressed SS and CS beams to the moving harmonic load is shown in Figure 15 and Figure 16, respectively. The curves shown in the figures are obtained for the case of the constant moving velocity, and with the excitation frequencies well below the fundamental frequencies of the beams. Only amplitude of the dynamic deflection is affected by the partial support, and it is lowered at a higher supporting parameter α, regardless of the boundary conditions. The computation has also been performed for other excitation frequencies, but the result is very much similar to that of the above-mentioned frequencies, and it is not shown herein.

4.5 Maximum dynamic deflection

As seen from Subsection 4.3, for a given foundation, there is a value of the moving velocity at which the dynamic deflection of the beams reaches a maximum value. This subsection investigates the influence of the moving velocity and the foundation stiffness on the maximum dynamic deflection of the beams. The maximum dynamic deflection is defined herein as the largest amplitude of the deflection when the load completely travels from the left-hand to the right-hand supports.

Figure 17 shows the moving velocity and the foundation stiffness versus the maximum dynamic deflection of the prestress SS beam for the case of an excitation frequency $\Omega = 20$ rad/s, and with different values of the second foundation parameters $k_2 = 0$ and $k_2 = 0.5$. As seen from Figure 17, for a given foundation stiffness, the maximum dynamic deflection of the SS beam reaches its peak at a certain value of the moving velocity, and this value is known as the critical velocity, Fryba (1972). This critical velocity, as seen from the difference between the two graphics shown in Figure 17, is affected by the presence of the second foundation parameter.

4.6 Significance of parameter $\mathbf{k_G}$

In addition to the traditional Winkler parameter k_W, the two-parameter foundation model employed in the present work is supplemented with the second parameter k_G representing stiffness of the shear layer. It is necessary to emphasize the significance of this parameter k_G on the dynamic response of the beams. To this end, the first foundation parameter k_1 is chosen to be 50, 100 and 200. The corresponding values of the Winkler modulus k_W are 9.375×10^5, 1.875×10^6 and 3.75×10^6 N/m^2, which belong to the typical stiffness of railway tracks, Thambiratnam and Zhuge (1996). Choosing an appropriate value for k_2 (that is for k_G) is not a simple task due to the lack of experimental data, Feng and Cook (1983). According to Feng and Cook (1983), $k_G = 6 \times 10^5$ N for a sandy clay foundation, and the extreme case for k_G is $\sqrt{4k_W EI}$, that is 2.1×10^8 N for the case $k_1 = 200$ and for the beam under investigation. The corresponding values of k_2 are 0.008 and 2.8. Choosing $k_2 = 0.1$, a value in range of the sandy clay foundation and the extreme case, we can numerically evaluate the effect of k_G on the natural frequency and the dynamic deflection of the beams. The numerical result reported below is for the case of the prestressed SS beam under a moving harmonic load with an excitation frequency $\Omega = 20$ rad/s, and with an axial force $Q = 0.2Q_b$.

Table 2 lists the natural frequency and the peak dynamic deflection of the SS beam resting on the traditional Winker foundation and on the two-parameter foundation with $k_2 = 0.1$ under the moving load. An increment of 3.16% in the natural frequency, and a reduction of 8.41% in the peak deflection with the presence of the second foundation parameter are observed for the case $k_1 = 50$. The difference in the natural frequency and the peak deflection decreases for the higher Winkler modulus foundation, and with $k_1 = 200$ the difference in the natural frequency reduces to only 1.6%, which is in range of the error of the finite element model. Consequently, the significance of the second foundation parameter strongly depends on the foundation stiffness, and in practice whether this parameter should be taken into account or not is decided by the concrete foundation.

k_1	k_2	ω_1 (rad/s)	difference (%)	D_{peak} ($\times 10^3$ m)	difference (%)
50	0	46.8709		8.2909	
	0.1	48.4014	3.16	7.5936	8.41
100	0	54.2710		5.5206	
	0.1	55.5981	2.38	5.1277	7.12
200	0	66.6500		2.7559	
	0.1	67.7350	1.60	2.5951	5.83

Table 2: Natural frequency and peak dynamic deflection of the prestressed SS beam resting on the Winkler foundation and on the two-parameter foundation with $k_2 = 0.1$ under a moving harmonic load ($\Omega = 20$ rad/s, $Q = 0.2Q_b$)

5 Conclusions

An investigation on the dynamic response of prestressed Timoshenko beams resting on a two-parameter foundation to a moving concentrated harmonic load has been conducted using the finite element method. A shear deformable

beam element taking the prestress and the foundation support was formulated and employed in the analysis using the direct integration Newmark method. The dynamic response of the simply supported and clamped-hinged beams has been computed at different values of the foundation stiffness, axial force, moving velocity and excitation frequency. The effects of the loading and foundation parameters on the response of the beams have been examined and discussed in detail. The main concluding remarks of the paper can be summarized as follows:

- The beam element formulated in the context of the field consistent approach and the numerical procedures employed in the present paper is accurate in computing the eigenfrequency and the dynamic response of the prestressed beams resting on the elastic foundation.
- The effect of the axial force on the dynamic response of the beams to the moving load is governed by the excitation frequency. With the excitation frequencies are considerably below the fundamental frequency, the compressive axial force reduces the bending stiffness of the beams as in the case of static analysis. Consequently, the dynamic deflection of the beams increases with an increment in the compressive axial force for these excitation frequencies. An opposite effect is observed in the case the excitation frequencies are remarkably higher than the fundamental frequency.
- The effect of the moving velocity is also governed by the excitation frequency, and the change in the dynamic deflection by the moving velocity strongly depends on the excitation frequency.
- There is a critical velocity at which the dynamic deflection of the beam reaches a peak value, and this critical velocity is governed by the foundation stiffness.
- The significance of the second foundation parameter strongly depends on the foundation stiffness, and in practice whether this parameter should be taken into account or not is decided by the concrete foundation.

Acknowledgement

The work presented in this paper has been financed in part by a National Program on the Fundamental Research.

Appendix

1. Interpolation functions for N_{wi} and $N_{\theta i}$ ($i = 1..4$) in equation (7)

$$\begin{aligned}
N_{w1} &= \frac{1}{(1+12\lambda)}\left(2\frac{x^3}{l^3} - 3\frac{x^2}{l^2} - 12\lambda\frac{x}{l} + 1\right)\\
N_{w2} &= \frac{1}{(1+12\lambda)}\left[\frac{x^3}{l^2} - (2+6\lambda)\frac{x^2}{l} + (1+6\lambda)x\right]\\
N_{w3} &= \frac{1}{(1+12\lambda)}\left(-2\frac{x^3}{l^3} + 3\frac{x^2}{l^2} + 12\lambda\frac{x}{l}\right)\\
N_{w4} &= \frac{1}{(1+12\lambda)}\left[\frac{x^3}{l^2} - (1-6\lambda)\frac{x^2}{l} - 6\lambda x\right]
\end{aligned} \tag{25}$$

and

$$\begin{aligned}
N_{\theta 1} &= \frac{6}{(1+12\lambda)}\left(\frac{x^2}{l^3} - \frac{x}{l^2}\right)\\
N_{\theta 2} &= \frac{1}{(1+12\lambda)}\left[3\frac{x^2}{l^2} - 4(1+3\lambda)\frac{x}{l} + (1+12\lambda)\right]\\
N_{\theta 3} &= \frac{6}{(1+12\lambda)}\left(-\frac{x^2}{l^3} + \frac{x}{l^2}\right)\\
N_{\theta 4} &= \frac{1}{(1+12\lambda)}\left[3\frac{x^2}{l^2} - 2(1-6\lambda)\frac{x}{l}\right]
\end{aligned} \tag{26}$$

2. Stiffness matrices in equation (13)

$$\mathbf{k}_B = \frac{1}{(1+12\lambda)l^3}EI\begin{bmatrix} 12 & & & \\ 6l & 4(1+3\lambda)l^2 & & sym. \\ -12 & -6l & 12 & \\ 6l & 2(1-6\lambda)l^2 & -6l & 4(1+3\lambda)l^2 \end{bmatrix} \tag{27}$$

$\mathbf{k}_F = \mathbf{k}_W + \mathbf{k}_G$; where

$$\mathbf{k}_W = \frac{l^3}{35(1+12\lambda)^2} k_W \mathbf{B} \quad ; \tag{28}$$

with

$$\mathbf{B} = \begin{bmatrix} \frac{(13+294\lambda+1680\lambda^2)}{l^2} & & & \\ \frac{(11+231\lambda+1260\lambda^2)}{6l} & \frac{(1+21\lambda+126\lambda^2)}{3} & & sym. \\ \frac{3(3+84\lambda+560\lambda^2)}{2l^2} & \frac{(13+378\lambda+2520\lambda^2)}{12l} & \frac{(13+294\lambda+1680\lambda^2)}{l^2} & \\ -\frac{(13+378\lambda+2520\lambda^2)}{12l} & -\frac{(1+28\lambda+168\lambda^2)}{4} & -\frac{(11+231\lambda+1260\lambda^2)}{6l} & \frac{(1+21\lambda+126\lambda^2)}{3} \end{bmatrix} \tag{29}$$

and

$$\mathbf{k}_G = \frac{l}{5(1+12\lambda)^2} k_G \mathbf{C} \quad ; \quad \mathbf{k}_Q = \frac{l}{5(1+12\lambda)^2} Q\mathbf{C} \tag{30}$$

with

$$\mathbf{C} = \begin{bmatrix} \frac{6(1+20\lambda+120\lambda^2)}{l^2} & & & \\ \frac{1}{2l} & \frac{2(1+15\lambda+90\lambda^2)}{3} & & sym. \\ -\frac{6(1+20\lambda+120\lambda^2)}{l^2} & -\frac{1}{2l} & \frac{6(1+20\lambda+120\lambda^2)}{l^2} & \\ \frac{1}{2l} & -\frac{(1+60\lambda+360\lambda^2)}{6} & -\frac{1}{2l} & \frac{2(1+15\lambda+90\lambda^2)}{3} \end{bmatrix} \tag{31}$$

3. Mass matrices $\mathbf{m}_{\dot{w}}$ and $\mathbf{m}_{\dot{\theta}}$ in equation (17)

$$\mathbf{m}_{\dot{w}} = \frac{l^3}{35(1+12\lambda)^2} \rho A \mathbf{B} \tag{32}$$

with matrix $\mathbf{B}$ given by equation (29), and

$$\mathbf{m}_{\dot{\theta}} = \frac{1}{5(1+12\lambda)^2} \rho I \begin{bmatrix} \frac{6}{l} & & & \\ \frac{1-60\lambda}{2} & \frac{2(1+15\lambda+360\lambda^2)l}{3} & & sym. \\ -\frac{6}{l} & -\frac{(1-60\lambda)}{2} & \frac{6}{l} & \\ \frac{(1-60\lambda)}{2} & -\frac{(1+60\lambda-720\lambda^2)l}{6} & -\frac{(1-60\lambda)}{2} & \frac{2(1+15\lambda+360\lambda^2)l}{3} \end{bmatrix} \tag{33}$$

References

Chen, Y.; Huang, Y.; Shin, C.: Response of an infinite Timoshenko beam on a viscoelastic foundation to a harmonic moving loads. *J. Sound Vibration*, 241, (2001), 809 – 824.

Cook, R.; Malkus, D.; Plesha, M.: *Concepts and applications of finite element analysis*. John Wiley & Sons, New York, U.S.A., 3rd edn. (1989).

Dugush, Y.; Eisengerger, M.: Vibrations of non-uniform continuous beams under moving loads. *J. Sound Vibration*, 254, (2002), 911 – 926.

Dutta, S.; Roy, R.: A critical review on idealization and modeling for interaction among soil-foundation-structure system. *Comput. Struct.*, 80, (2002), 1579 – 1594.

Feng, Z.; Cook, R.: Beam elements on two-parameter elastic foundations. *J. Engrg. Mech.*, 109, (1983), 1390 – 1402.

Fryba, L.: *Vibration of solids and structures under moving loads*. Academia, Prague, Czech Republic (1972).

Géradin, M.; Rixen, R.: *Mechanical vibrations. Theory and application to structural dynamics*. John Wiley & Sons, Chichester, U.K., 2nd edn. (1997).

Ghali, A.; Neville, A.: *Structural analysis. A unified classical and matrix approach*. E & FN Spon, London, U.K., 3rd edn. (1995).

Hetényi, M.: *Beams on elastic foundation*. The University of Michigan Press, Ann Arbor, U.S.A. (1946).

Kien, N. D.: Post-buckling behavior of beam on two-parameter elastic foundation. *Int. J. Struct. Stab. Dynam.*, 4, (2004), 21 – 43.

Kocatürk, T.; Şimşek, M.: Vibration of viscoelastic beams subjected to an eccentric compressive force and a concentrated moving harmonic force. *J. Sound Vib.*, 291, (2006), 302 – 322.

Luo, Y.: Explanation and elimination of shear locking and membrane locking with field consistence approach. *Comput. Methods Appl. Mech. Engrg.*, 162, (1998), 249– 269.

Maple: *Language reference manual*. Spring-Verlag, New York, U.S.A. (1991).

Naidu, N.; Rao, G.: Vibrations of initially stressed uniform beams on a two-parameter elastic foundation. *Comput. Struct.*, 57, (1995), 941 – 943.

Rao, G.: Large-amplitude free vibrations of uniform beams on Pasternak foundation. *J. Sound Vib.*, 263, (2003), 954 – 960.

Shames, I.; Dym, C.: *Energy and finite element methods in structural mechanics*. McGraw-Hill, New York, U.S.A. (1985).

Thambiratnam, D.; Zhuge, Y.: Free vibration analysis of beams on elastic foundation. *Comput. Struct.*, 60, (1996), 971 – 980.

Timoshenko, S.; Young, D.; Weaver, W.: *Vibration problems in engineering*. John Wiley, New York, U.S.A., 4th edn. (1974).

Yokoyama, T.: Vibration analysis of Timoshenko beam-column on two-parameter elastic foundation. *Comput. Struct.*, 61, (1996), 995 – 1007.

Address: Dr. Nguyen Dinh Kien, Institute of Mechanics, Vietnam Academy of Science and Technology, 224 Doi Can Street, Hanoi, Vietnam.
email: ndkien@imech.ac.vn